

# PersiST: Robust Identification of Spatially Variable Features in Spatial Omics Datasets via Topological Data Analysis

James Boyle<sup>1\*</sup>, Gregory Hamm<sup>2</sup>, Eleanor Williams<sup>3,4</sup>, Robin JG Hartman<sup>1</sup>, Magnus Söderburg<sup>1</sup>, Ian Henry<sup>1</sup>, and Michael Casey<sup>1</sup>

<sup>1</sup>Data Science and AI, Translational Science & Experimental Medicine, Research and Early Development, Cardiovascular, Renal and Metabolism, Biopharmaceuticals R&D, AstraZeneca, Cambridge, UK

<sup>2</sup>Integrated Bioanalysis, Clinical Pharmacology and Safety Sciences, Biopharmaceuticals R&D, AstraZeneca, Cambridge, UK

<sup>3</sup>Cambridge Stem Cell Institute, University of Cambridge, Cambridge, UK

<sup>4</sup>Predictive AI and Data, Clinical Pathology and Safety Sciences, Biopharmaceuticals R&D, AstraZeneca, Cambridge, UK

<sup>5</sup>Cardiovascular Renal and Metabolism Pathology, Clinical Pharmacology and Safety Sciences, Biopharmaceuticals R&D, AstraZeneca, Cambridge, UK

\*Correspondence to james.boyle@maths.ox.ac.uk

## Abstract

Spatial transcriptomics studies are becoming increasingly large and commonplace, necessitating the analysis of a large number of spatially resolved variables. With spatial transcriptomics data sets typically containing data on thousands of different genes, on increasingly large numbers of samples, there is a need for bioinformatics tools that enable the comparison of spatial structure across large numbers of variables. Here we present PersiST, an exploratory tool that uses topology to automatically compute a continuous measure of spatial structure for each gene in a spatial transcriptomics sample. This quantification can be used for analytical tasks such as spatially variable gene identification, or searching for spatial differences in the expression of a gene between samples. We use PersiST to derive biologically meaningful insights into two public spatial transcriptomics data sets, and we experiment with applying PersiST to a spatial metabolomics data set, making use of PersiST's non-parametric approach to enable application across different measurement types. Our work showcases the advantages of using a continuous quantification of spatial structure over p-value based approaches to SVG identification, the potential for developing unified methods for the analysis of different spatial 'omics modalities, and the utility of persistent homology in big data applications.

## 1 Introduction

Spatial transcriptomics experiments measure gene expression in 2-dimensional space, up to the resolution of a supra-cellular well, cell, or subcellular location [1, 2]. A common task in analysing spatial transcriptomics data is to identify genes that exhibit spatial structure to their expression, commonly referred to as *Spatially Variable Genes* (SVGs) [3, 4]. The majority of existing

SVG identification methods are based on null hypothesis rejection, with a null hypothesis corresponding to no spatial variability [4, 5]. (Adjusted) p-values are then used to determine which genes are Spatially Variable (SV).

Hypothesis rejection approaches treat spatial variability as a binary quantity reflective of some underlying biological process. We instead follow the approach taken in [6] and consider the degree of spatial structure in a gene's expression as a continuous descriptive quantity. This approach enables further analysis beyond simply declaring genes as SV or not SV, such as comparing spatial structure in gene expression within or between samples. Current methods for SVG identification show large discrepancies in the number of SVGs they identify, and the spatial expression patterns they typically detect [3].

Here we introduce a new method, *PersiST* (Persistent expression in Spatial Transcriptomics), that quantifies spatial variability via the topological activity in a gene's expression pattern [7]. Our methodology is based on quantifying the number and significance of 'hotspots' in a gene's expression, taking the presence of one or more distinct regions of differential gene expression as indicative of spatial structure. PersiST is able to detect a broad range of spatial patterns and is robust to variance in tissue morphology. Moreover, PersiST makes no assumptions about the statistical distribution of gene expression or gene count data, being instead based purely on the data's topology. This enables PersiST to be easily applied to other spatial 'omics modalities, and we show this by using PersiST to analyse a spatial metabolomics data set [8].

Although there exist other methods that perform SVG identification via continuous spatial structure quantification, PersiST is more robust than such methods, identifies novel patterns of spatial structure not picked up on by [6], and produces a score that can be used for additional analytical tasks.

Methodologically, PersiST is a novel application of Topological Data Analysis (TDA) and in particular of Persistent Homology (PH) [9]. PH has previously been used for analysing spatial structure in spatial transcriptomics data sets and other biological settings [10, 11, 12], but as far as the present authors are aware, PersiST is one of the first "big data" applications of PH, in which PH is used to automatically perform some analytical task on a large number of spatially resolved variables, the output of which does not involve any manual inspection of the PH outputs. In other words, PersiST can be comfortably used by a practitioner without any knowledge of PH or TDA. We thus hope this work highlights not just the utility of PH for analysing full transcriptome spatial transcriptomics data sets, but also the potential of PH for use in other high dimensional settings.

The paper is structured as follows. We first provide a brief overview of the methodology and outputs of PersiST. We then illustrate PersiST's capabilities on a kidney disease data set - we showcase some types of spatial structure detected by PersiST, and we use the spatial structure quantification provided by PersiST to highlight genes that show spatial differences in expression between Acute Kidney Injury and Chronic Kidney Disease samples [13]. Next we use PersiST to analyse a myocardial infarction data set [14], and finally we show how PersiST can be used to analyse a spatial metabolomics sample, illustrating how PersiST's methodology can be extended to other spatial 'omics modalities.

We present PersiST as an exploratory tool. That is, given spatial transcriptomics data on a large number of genes, a practitioner can use PersiST to triage the data down to a smaller number of genes which, for example, display notable spatial structure, or differences in spatial structure between subgroups, and subject these genes to further analysis.

Throughout, we compare PersiST to a range of popular SVG identification methods - SpatialDE [4], SPARK-X [5], and Sepal [6]. These were chosen to represent the diverse range of methodologies employed by SVG identification methods. Comparison and benchmarking of spatial feature selection methods is complicated by a lack of ground truth, the diversity in the types of spatial patterns genes can exhibit, and the wide range of different methodologies used for SVG identification by existing methods. Therefore, our comparisons are restricted mainly

to assessing the overlap in SVGs called by each method, with some manual inspection of those genes called differently.

## 2 Method Overview

The PersiST algorithm takes as input the spatially resolved expression of a large number of genes over a fixed set of co-ordinates. For each gene, PersiST computes a single number, the *Coefficient of Spatial Structure* (CoSS), that quantifies the amount of spatial structure in that gene's expression pattern (figure 1a). In this section we provide an overview of how PersiST computes the CoSS for a single gene (figure 1); for a more complete description see *Methods*.

The CoSS for a gene is computed by looking at the number and significance of expression 'hotspots' in the tissue - regions of substantially higher gene expression than surrounding tissue.

For each gene, PersiST computes a smoothed version of the gene's expression (figure 1b, [9]). Intuitively, for SVGs the surface plot of this smoothed expression should be more "hilly". PersiST then looks at *level sets* of the smoothed expression - regions of the underlying tissue where the smoothed expression exceeds a certain threshold (figure 1e). PersiST considers the level sets over a continuous range of thresholds, from the maximum value of the smoothed expression down to zero. Regions of higher expression will be present in the level set at higher thresholds than regions of lower expression. As the threshold varies from its maximum down to zero, a region of the tissue that has significantly higher expression than the surrounding tissue will appear (be "born") as a disconnected component in the level set at a high threshold, and will only merge with the rest of the tissue ("die") at a low threshold, when the surrounding tissue appears in the level set [9]. By contrast, a region with expression only slightly higher than the surrounding tissue will die shortly after it is born. By looking at the "lifetime" of a hotspot - the difference between its birth and death threshold - we can measure the significance of the hotspot, and distinguish spatial signal from spatial noise.

The information from this level set analysis is neatly summarised in a *barcode diagram* (figure 1c, [9]), consisting of a bar for each hotspot from its birth to death threshold - a coarse but tractable summary of the spatial structure of the gene's expression. The CoSS is computed as the  $L^2$ -norm of the barcode, i.e. by summing up the squared lengths of each bar [15, 16]. The CoSS is thus a summary of the number and lifetimes of a gene's expression hotspots.

The CoSS for each gene can then be used for downstream tasks that involve comparing the spatial structure of different gene expression patterns. For example, SVG identification can be done by declaring all genes with a CoSS above some cutoff to be SV. PersiST automatically selects a threshold for a given sample (figure 1d), but a practitioner-selected cutoff can also be used if desired.

## 3 Results

We use PersiST to analyse two publicly available Visium spatial transcriptomics data sets [13, 14], and one internal Mass Spectrometry Imaging (MSI) data set. We also compare the performance of SpatialDE, SPARK-X and Sepal on the spatial transcriptomics data sets. The spatial transcriptomics data sets were chosen as they both contain multiple samples of varying, well-defined disease phenotypes, and within each data set all samples were collected using the same data generation protocols. The two data sets also represent two "ends" of the spatial transcriptomics spectrum with respect to data complexity: [13] contains samples with highly variant and quite complex morphology, where the expression was measured over a small number of relatively large wells, whereas [14] mostly contains samples with comparatively simple tissue morphology, with gene expression resolved over a large number of smaller (though still supra-cellular) wells.

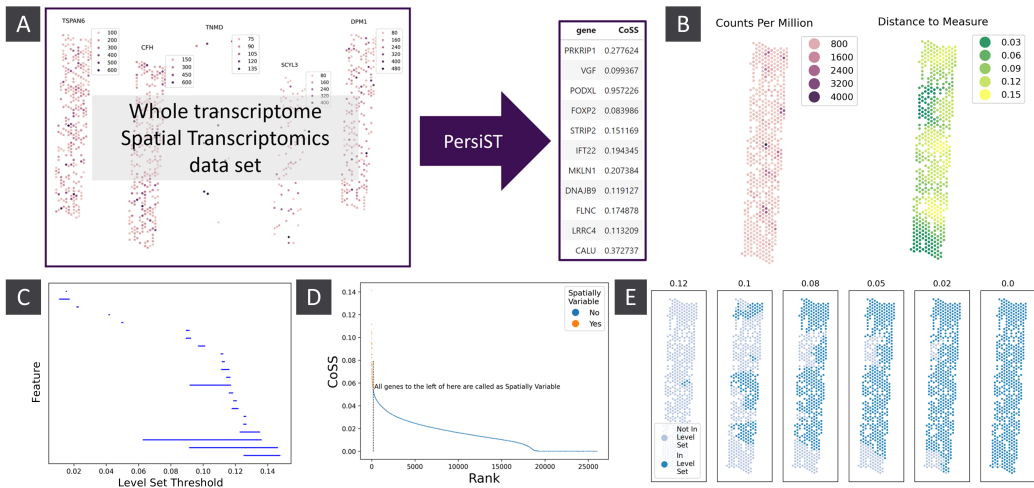


Figure 1: An illustration of the methodology behind PersiST. a) Illustration of the input and output of PersiST. PersiST takes as input spatial ‘omics data on some large number of features, and outputs for each gene a single number quantifying the amount of spatial structure in that gene’s expression. b) Original expression data (in counts per million) and the smoothed expression used by PersiST for the gene PODXL in kpmp sample 30-10125. c) The barcode diagram for the 0-dimensional persistent homology of the upper star filtration generated by the smoothed expression in panel b. d) Level sets of the smoothed expression in panel b, at various thresholds. e) A plot of the CoSS and rank for each gene in sample 30-10125. The CoSS cutoff for declaring a gene as spatially variable is automatically selected based on the curvature of the CoSS-Rank curve.

## Using PersiST to Analyse Kidney Disease Spatial Transcriptomics Data

We applied PersiST to spatial transcriptomics data from the Kidney Precision Medicine Project (KPMP, [13]). This data consists of 6 Acute Kidney Injury (AKI) and 8 Chronic Kidney Disease (CKD) samples, with expression data on 26027 genes resolved to  $55\mu\text{m}$  wells. The number of wells varies from 317 to 787 across the samples. The tissue samples display distinct morphological variation, including some with highly irregular shapes or with multiple disconnected components (supplementary figure 4). Such variation presents a significant challenge for producing comparable SVG identification analyses between the different samples.

The amount of SVGs identified by PersiST in each sample based on the automatically selected CoSS-cutoff ranged from 62 to 353. There was no correlation between the number of SVGs identified and the number of wells in the sample (table 1, supplementary figure 5a).

Table 1 provides summary statistics on the number of SVGs identified by each of the comparison methods in each of the kpmp samples, plotted in supplementary figure 5a against the number of wells in each sample. Notably, 1) SpatialDE and SPARK-X, the two methods based on null hypothesis rejection, consistently call more genes as SV than PersiST or Sepal, the two methods based on continuous quantification of spatial structure, 2) SpatialDE and SPARK-X exhibit much more variability in the number of SVGs called, with SPARK-X exhibiting a substantial correlation between the number of SVGs and the number of wells in a sample, and 3) Sepal consistently identifies less SVGs than PersiST, for some samples only calling a single digit number of genes as SV.

Spatial feature identification is effectively a form of triage, reducing a large initial number

method	min	max	standard deviation	correlation with number of wells
PersiST	80	332	61.0	-0.11
Sepal	4	93	27.3	0.21
SpatialDE	104	1014	282.9	0.20
SPARK-X	124	3886	1205.8	0.51

Table 1: Summary statistics for the number of SVGs called in each of the kpmp samples, for each of the comparison methods. Correlations shown are spearman correlation.

of features down to a smaller number with spatial structure for further analysis. Calling a excessively high number of features as SV increases the downstream burden on the practitioner, whilst calling too few features as SV risks missing out on important biological signal. We argue PersiST hits a “sweet spot” with respect to the number of features called as SV, and exhibits greater consistency in the number of features called as SV. Moreover, the use of continuous scores enables a practitioner to triage with greater fidelity the features they wish analyse further, by varying the score cutoff for a feature to qualify as SV.

### SVG Examples

To illustrate the range of spatial structures detected by PersiST, we exhibit a couple of sets of SVGs identified by PersiST, presented in groups with co-localised expression patterns, detected manually using hierarchical clustering on the list of SVGs produced by PersiST. Once PersiST had reduced the number of genes down to a small number of those with notable spatial structure, simple clustering methods were sufficient to pick out groups of SVGs with similar expression patterns. Our focus is on the ability of PersiST to detect and quantify spatial structure, but for the results in this section we give some light biological interpretation.

### PersiST Detects Co-Localised Genes Expressed in the Glomeruli

The type of spatial structure PersiST is most evidently able to detect consists of multiple distinct regions of high expression (“hotspots”) surrounded by a background level of lower expression.

In one of the AKI samples we identified a group of SVGs that were highly expressed in regions of the tissue corresponding to glomeruli (figure 2a), as verified by pathologist review of the accompanying H&E images. Some of these, such as PODXL, are well-known glomerular marker genes, whilst others have not been reported as such. In particular, IFI27 is an interferon related gene, indicating the presence of immune activity at the glomeruli.

SpatialDE and SPARK-X also identified the genes in figure 2a as SV (except SpatialDE failed to call IGFBP5 as SV), but Sepal failed to identify any of these genes as spatially variable.

### A Single Highly Expressed Well

Another common type of spatial structure in the kpmp data set consists of a single highly expressed well against a background of much lower expression. Whilst such spatial variation is comparatively simple, it is important that such genes are correctly flagged as SV by an automatic SVG identification process.

Supplementary figure 6 shows a collection of PersiST identified SVGs that are all highly expressed in the same well.

The two p-value based benchmark methods struggled here. SpatialDE failed to call COX7B, RNF207 and NOC2L as SV, and SPARK-X, despite calling vastly more genes as SV than

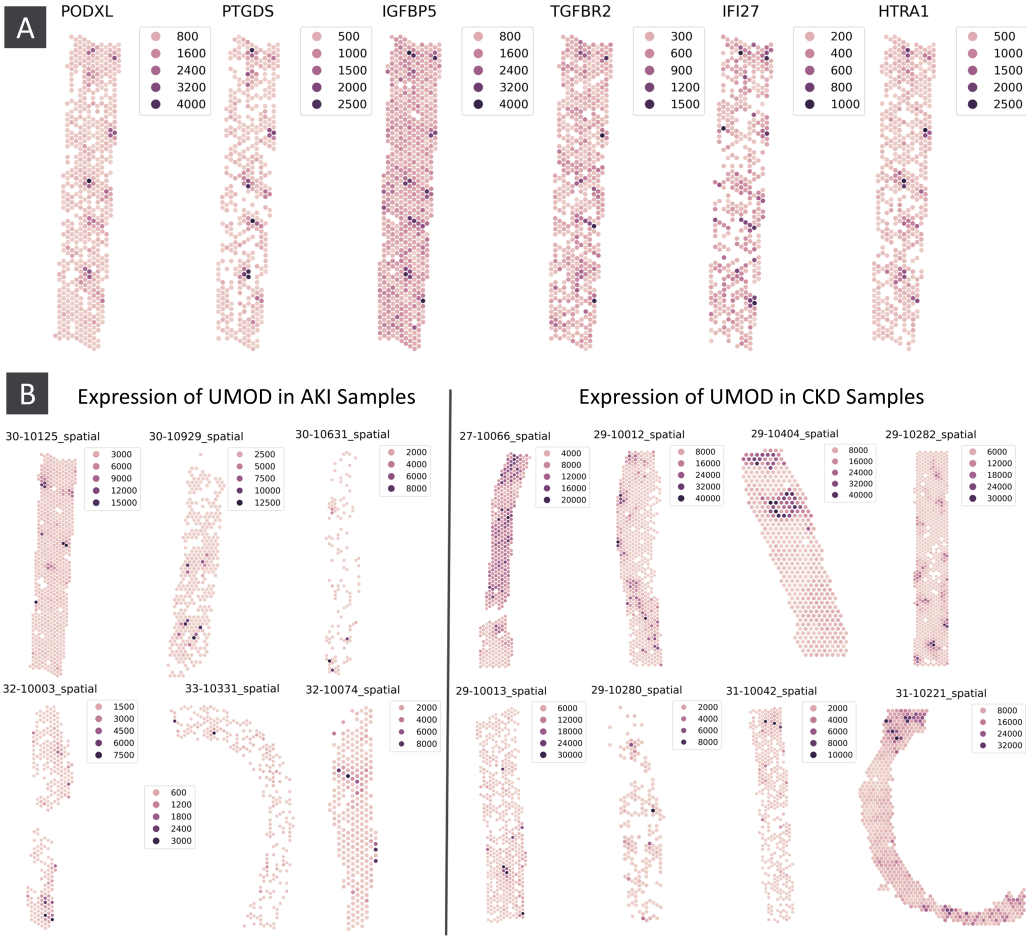


Figure 2: a) Co-expression of PODXL, PTGDS, IGFBP5, TGFBR2, IFI27, HTRA1 in kpmp sample 30-10125 (AKI) at locations corresponding to glomeruli in the tissue. Genes all identified as spatially variable by PersiST . b) Expression of UMOD in the AKI and CKD kpmp samples.

PersiST (1161 compared to 188), failed to call RNF207 or NOC2L as SV. Sepal also failed to call any of these genes as SV.

### CoSS Scores Capture Structural Breakdown in CKD

The continuous quantification of spatial structure provided by PersiST can be used for additional analysis beyond identifying spatially variable genes.

One such task is detecting differences in the spatial structure of a gene's expression between sample subgroups. We computed for each gene the difference in mean CoSS between the AKI and CKD samples in our cohort, and inspected the list of genes for which this difference was highest.

The uromodulin encoding gene UMOD (a marker of kidney tubules) had the highest mean CoSS difference between the AKI and CKD samples. In the AKI samples the expression of UMOD is generally concentrated in a small number of very well-defined regions of high expres-

	PersiST	SpatialDE	Sepal	SPARK-X
PersiST	188	58 (0.21)	0	154 (0.13)
SpatialDE	58 (0.21)	144	1 (0.01)	116 (0.10)
Sepal	0	1 (0.01)	69	0
SPARK-X	154 (0.13)	116 (0.10)	0	1157

Table 2: Number of genes mutually identified as spatially variable by different pairs of SVG identification methods in kpmp sample 30-10125. Values in brackets are normalised by the number of genes called as spatially variable by either method. Diagonal entries are the number of SVGs called by each method.

sion, whereas in the CKD samples the expression pattern of UMOD is much more diffuse, with less well-defined regions of high and low expression (figure 2b).

Progression of kidney disease is characterised by a general breakdown in the physical structure of the organ. Using PersiST we can see, automatically detect, and quantify this structural breakdown directly from the spatial transcriptomics data.

We also inspected the mean differences in Sepal scores, and adjusted p-values provided by SpatialDE and SPARK-X. Although these quantities were not originally proposed for this application, we perform this comparison to see if the CoSS is novel in this respect. For the Sepal score, we also consider this analysis a natural extension for continuous measures of spatial structure. In our analysis, UMOD only had the 6163<sup>th</sup>, 6352<sup>th</sup>, and 234<sup>th</sup> greatest difference according to the Sepal score, SpatialDE q-values and SPARK-X adjusted p-values; moreover, those genes with the greatest mean difference did not display any consistent notable difference in spatial structure between the AKI and CKD samples (supplementary figure 7).

### Overlap Between Different SVG Identification Methods

We investigated the overlap between the SVGs identified by PersiST, SpatialDE, SPARK-X and Sepal. Table 2 gives the number of genes mutually identified as SV by each pair of methods, in the kpmp sample shown in figure 2a, along with a normalised version of this number divided by the total number of genes called as SV by either method. PersiST displays some overlap with the comparator methods, whilst identifying plenty of novel SVGs. There is also a substantial amount of difference even between the established SVG identification methods, this lack of agreement between SVG identification methods has been observed previously [3].

The overlap numbers for the other samples are given in supplementary data 1, they do not differ qualitatively from the data for the sample presented here.

### 3.1 Applications to Myocardial Infarction Data

We use PersiST to analyse a spatial transcriptomics data set consisting of samples from multiple physiological zones of the heart from myocardial infarction and control patients [14]. These samples contain expression on 16272 genes resolved to between 1890 and 4659 10 $\mu$ m wells, with samples from the borderzone, fibrotic zone, ischaemic zone and remote zone, as well as control samples.

We include this analysis to demonstrate the general applicability of PersiST to spatial transcriptomics data. PersiST performs favourably compared to the benchmarked methods with respect to consistency in number of SVGs called, and the correlation between the number of SVGs called and the number of wells in each sample (supplementary table 3, supplementary figure 5b).

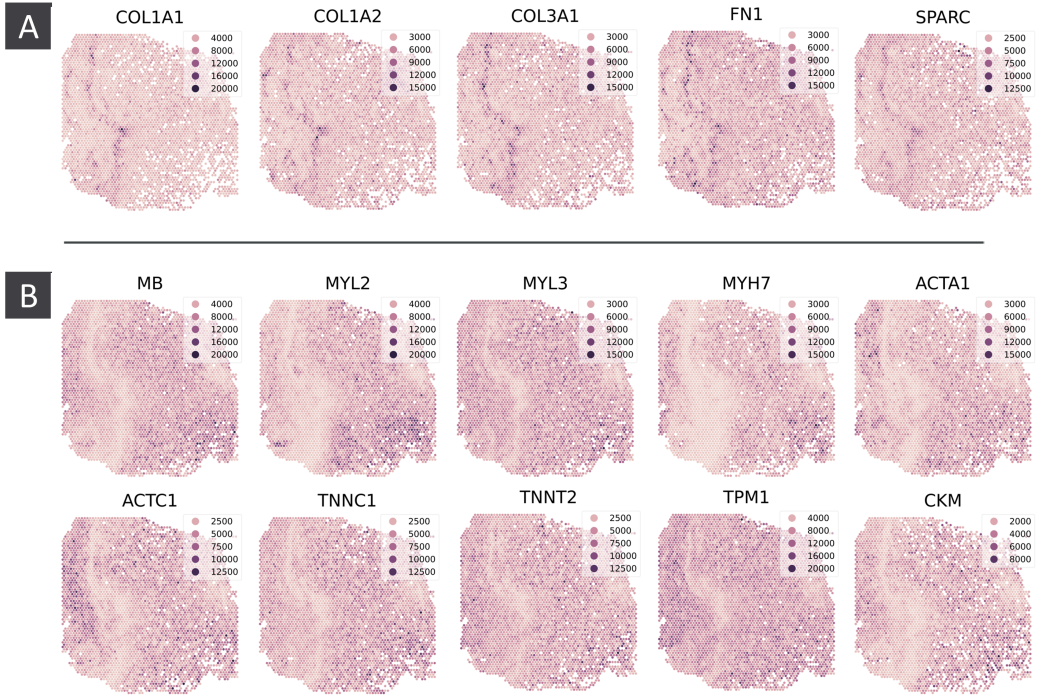


Figure 3: Select PersiST-SVGs from myocardial infarction sample AKK003-157775 (Ischaemic Zone) - a) Co-expression of COL1A2, COL1A1, COL3A1, FN1 and SPARC. b) Co-expression of MB, MYL2, MYL3, MYH7, ACTA1, ACTC1, TNNC1, TNNT2, TPM1 and CKM. Genes in panel b display a noticeable drop in expression in the same region where the genes in panel a are highly expressed.

### Spatial Transcriptomics Provides Additional Insight into Cardiac Fibrosis

PersiST identified five SVGs in an ischaemic zone sample all co-localised with COL1A2 (figure 3a). COL1A2 has previously been identified as a driver of cardiac fibrosis [17], and in [18] the authors use tomo-seq [19] to identify a group of genes whose differential regulation correlates with COL1A2 across an infarcted mouse heart. This group includes COL1A1, COL3A1, FN1 and SPARC; here we are able to verify the co-expression of these genes with COL1A2 at finer spatial resolution.

PersiST additionally identified a group of SVGs which display a distinct drop in expression in the same region in which the above genes are highly expressed (figure 3b). In persistent homology, such “voids” in expression also contribute to the CoSS score [9]. Using PersiST and spatial transcriptomics, we are able to add additional insight into cardiac fibrosis beyond other methods.

Sepal fails to identify any of the genes discussed in this section as SV. SPARK-X and SpatialDE identify all these genes as SV, but SpatialDE does so by calling every gene as SV.

### 3.2 Applications to Spatial Metabolomics Data

Although PersiST was developed for application to spatial transcriptomics data, it is agnostic as to the type of measurement recorded at each location, simply using persistent homology to quantify spatial structure in a weighted point cloud. Beyond spatial transcriptomics, there are

many other biomedical data modalities that can be presented in this format. PersiST does not make any assumptions about the statistical distribution of gene expression data, so we experimented with applying PersiST to detect spatial structure in other modalities, making no changes to the underlying methodology.

In this section we use PersiST to analyse a spatial metabolomics (Mass Spectrometry Imaging, MSI) sample [20]. Persistent homology remains effective as an exploratory tool for highlighting metabolites with notable spatial structure. Whilst PersiST was robust to differences in the statistical properties of metabolite intensity data compared to gene expression data, the larger size (in terms of the number of points at which metabolite intensity was measured) of the sample we analysed necessitated a different level of smoothing. Additionally, converting the continuous CoSS values into a binary call of spatial variability was complicated by the qualitatively different CoSS-rank profile compared to the spatial transcriptomics samples (figure 1d, supplementary figure 1c). These points highlight some of the finer workings of PersiST, and the difficulties of translating a data analysis methodology between spatial modalities. We discuss them further in *supplementary analysis*. We hope that this section highlights both opportunities and challenges for developing unified methods for the analysis of different types of spatial ‘omics data.

### Spatial Metabolomics Data

In spatial transcriptomics, at each spatial location we measure the *expression of genes*. In MSI, we measure the *intensity of metabolites*. More specifically, once a grid of pixels on the tissue is decided, within each pixel the molecules of the tissue are ionised, and a mass spectrum is collected. Post data collection, computational software is used to select individual mass-to-charge ( $m/z$ ) peaks, and the intensity of each  $m/z$  peak at each pixel is reported. It is at this point that the data is analogous to spatial transcriptomics data, where each feature has a measurement at each of a shared set of co-ordinates. We refer to the MSI features by their  $m/z$  ratios. The molecular identity of a specific  $m/z$  value can be determined by tandem MS (MS/MS) fragmentation, or by matching its intact mass to databases of known molecular masses within a certain mass error range (expressed in parts per million, ppm) [8].

For the sample we analyse in this section, mass spectrometry imaging was used to measure metabolite intensity on a fresh frozen rat testis at a spatial resolution of  $40\mu\text{m}$ .

### PersiST Highlights Metabolites Providing Insight into Spermatogenesis

Metabolites 600.5148, 602.5077, and 601.51505 (figure 4b, supplementary figure 1a) were all flagged by PersiST as SV, and have co-localised regions of high intensity. Pathologist review of the accompanying H&E slide (figure 4a,e,f) confirmed that these metabolites have high intensity in regions of the tissue corresponding to seminiferous tubules in the early/mid stage of spermatogenesis. Spermatogenesis occurs continuously and repeatedly in the germinal epithelium of the seminiferous tubules where these metabolites can be found. The  $m/z$  features flagged by PersiST as tubular maturation markers are isotopes from the same molecular species, a ceramide identified as Cer(36:1) and detected as chloride adduct,  $[\text{M}+\text{Cl}]^-$  with a mass accuracy of 3.3 ppm compared to theoretical  $m/z$  ( $m/z$  ratios identified using the Human Metabolite Database [21]). Levels of such sphingolipids, particularly ceramide levels, have been observed changing during the maturation phase of spermatogenesis [22].

Metabolite 730.59083 also shows high intensity in similar regions but is present exclusively round the edges of the tubules (figure 4c), whilst Spatially Variable Metabolites (SVMs) such as 838.55351 displayed hotspots of high intensity exclusively inside the tubules (figure 4d).

Using PersiST, MSI and histology data, we were able to identify local metabolic perturbations within our sample, and link the  $m/z$  features identified by PersiST with a specific biological process.

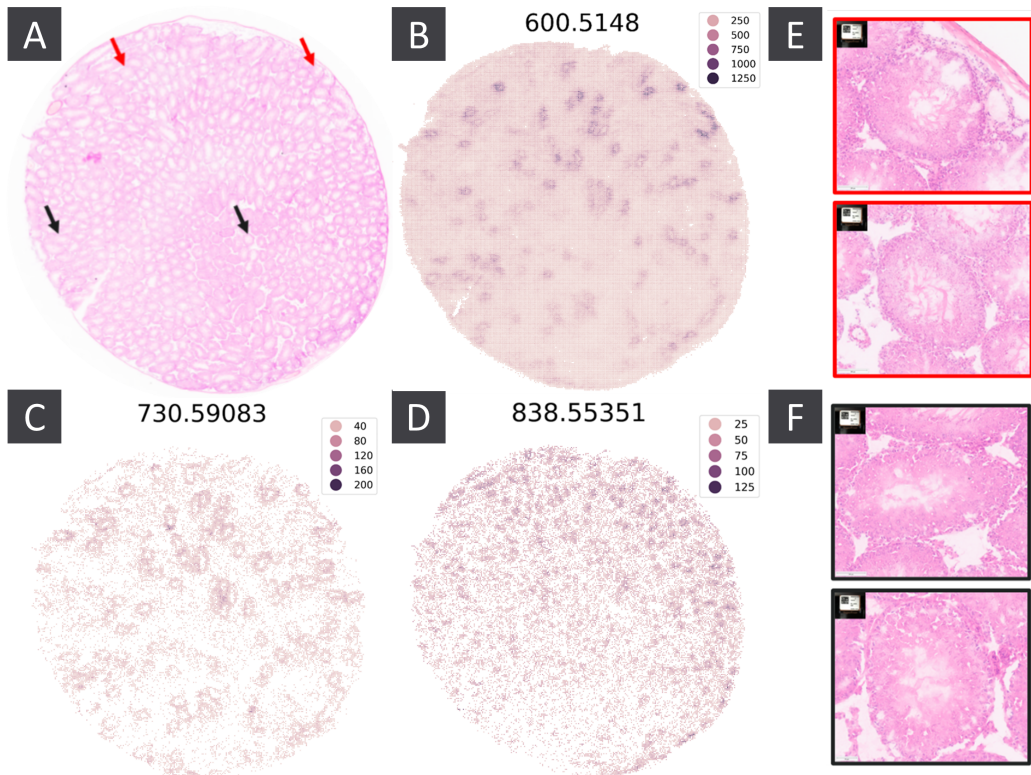


Figure 4: a) H&E slide for the MSI sample. Red and black arrows point to example seminiferous tubules in the early/mid and late stage of spermatogenesis respectively. b,c,d) Spatial intensity of select PersiST identified SVMs. e,f) Zoomed in H&E image for the regions indicated by the red and black arrows in panels a and b.

## 4 Discussion

We have developed an automatic procedure using topology to compute, from spatial ‘omics data on a large number of features, a continuous measure of spatial structure for each feature. We have shown this measure to be a useful exploratory tool for analysing spatial ‘omics data sets, with demonstrated applications to feature selection and differential spatial expression analysis in multiple spatial ‘omics data modalities across different biological settings.

Using spatial structure scores, rather than null hypothesis rejection, better reflects the status of “spatial variability” as a descriptive property of biological systems rather than an intrinsic binary biological quantity. Moreover, continuous scores are a valuable quantity that can be useful for multiple analytical tasks. Developing a method for computing such scores based on principled notions of spatial structure, rather than statistical properties of gene expression data, enabled our score to be meaningful across multiple spatial ‘omics modalities.

As far as the authors are aware, our work is also a novel application of persistent homology to produce an automatic method for analysing big data, that requires no knowledge of persistent homology to be used by a practitioner. That a simple “out of the box” application of persistent homology produced such useful results for multiple spatial ‘omics modalities indicates its broad utility for analysing such data.

## 5 Methods

We give in full detail the process of going from the output of a spatial transcriptomics experiment to a CoSS for each gene, and a binary call of which genes are spatially variable.

The output of a spatial transcriptomics experiment may be modelled as a collection of weighted point clouds, one for each gene. The data for a single sample consists of the co-ordinates  $(x_i, y_i)_{i=1:n_{\text{wells}}}$  of each well, and for each gene  $g$  a sequence of weights  $(w_i)_{i=1:n_{\text{wells}}}$ , where  $w_i$  is the expression of  $g$  in well  $i$ . To enable robustness to tissue morphology, the wells are assumed to lie on a regular hexagonal or square network structure (*supplementary methods*, supplementary figure 2a,b). PersiST automatically aligns the given well co-ordinates to a network structure (*supplementary methods*).

### Using Distance to Measure for Smoothed Expression Profiles

We detail how we compute the CoSS for a given gene  $g$ . We first normalise the weights at each well such that  $\sum_i w_i = 1$ , so that the spatial expression of  $g$  defines a weighted point cloud specifying a probability distribution over the observed wells.

For robustness, PersiST operates on a smoothed version of the gene's expression. We use a modified form of the *Distance to Measure* of a point cloud. For a probability density  $\rho$  on  $\mathbb{R}^2$ , the distance to measure of a point  $p \in \mathbb{R}^2$  is defined in [23] as

$$\text{dtm}(p; m) = \frac{1}{m} \int_0^m \delta_a^2(x) da$$

for some pre-defined  $m \in (0, 1)$ , where  $\delta_a(x) = \inf\{r > 0 : \mathbb{P}_\rho(B(x, r)) > a\}$  is the minimal radius of a ball around  $x$  covering at least  $a$  of the mass of  $\rho$ .

If  $\rho$  is the empirical density of a point cloud  $(x_i)_{i=1:n} \subseteq \mathbb{R}^2$ , the distance to measure is given by

$$\text{dtm}(p; m) = \frac{1}{k} \sum_{i=1}^k \|p - x^{(i)}\|^2 \quad (1)$$

where  $k = \lfloor mn \rfloor$ , and  $x^{(i)}$  is the  $i^{\text{th}}$  nearest point to  $p$  [9] (we will be evaluating dtm at each well, so  $p = x_i$ ,  $x^{(1)} = p$ , and  $\|p - x^{(1)}\| = 0$ ). This is the average squared distance from  $p$  to its  $k$  nearest neighbours, where  $k$  is minimal such that the combined mass on the neighbours is at least  $m$ . Note that the definition of  $\text{dtm}(p; m)$  depends on the co-ordinates of all points in the point cloud, but we suppress this in the notation.

The distance to measure preserves many desirable features of a classic density estimator, but is more robust to noise in the input data, and has been observed to be more robust when used as an input to persistent homology [9].

The smoothing function used by PersiST is an extension of (1) to the case of a weighted point cloud.

### PersiST's Smoothed Expression

The smoothing function used by PersiST is a modified version of the distance to measure of a point cloud. The smoothing function used by PersiST is given by

$$\text{dtm}(p; m) = \frac{1}{k} \sum_{i=1}^k d_i^2 \quad (2)$$

where  $k = \min \left\{ N : \sum_{i=1}^N w^{(i)} \geq m \right\}$ , and  $d_i$  is the distance from the central vertex to the  $i^{\text{th}}$  nearest neighbour vertex in an infinite radial network of the same type as the data, with  $d_1 = 0$  (figure 5).

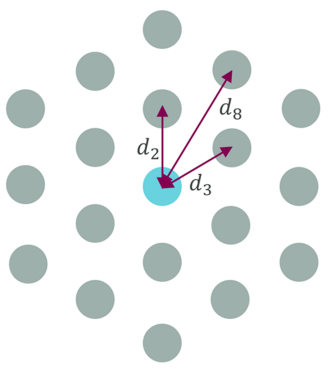


Figure 5: Figure illustrating the 2<sup>nd</sup>, 3<sup>rd</sup>, and 8<sup>th</sup> shortest distances between a central node (light blue) and the surrounding nodes (grey) in a hexagonal grid.  $d_1 = 0$ , as the distance from the light blue node to itself.

The upper limit of the sum is still the number of nearest neighbour wells needed to reach a combined mass of  $m$ , but this will now vary depending on  $p$ . The network distances  $d_i$  are used to control for the fact that the sequence of distances  $(||p - x^{(i)}||)_i$  will increase more quickly for wells near the edge or near holes in the tissue, than for wells in the middle of the tissue, leading to artificially higher values of  $\text{dtm}(p; m)$ . By using network distances, we treat every well like it is right in the middle of the tissue, effectively re-arranging the wells near  $p$  needed to reach a mass of  $m$  such that they surround  $p$  in a regular network structure, and computing  $\text{dtm}(m; p)$  as if this were what the actual data looked like.

When we refer to distance to measure, smoothed expression, or  $\text{dtm}(p; m)$  below, we shall mean the quantity defined in (2).

### Using Persistent Homology to Compute CoSS Values

This section assumes a basic understanding of persistent homology (PH). For a brief introduction to PH, see [24].

We now have a collection of wells with co-ordinates  $(x_i)_i$  and smoothed expression values  $\text{dtm}(x_i; m)$ , producing a smoothed surface plot of the gene's expression. The smoothed expression is currently lower in regions of higher original expression, so we first invert this surface about its median, replacing  $\text{dtm}(x_i; m)$  with  $z_i = \max\{\text{dtm}(x_j; m)\}_{j=1:n} - \text{dtm}(x_i; m)$ . This is to fit our intuition that the smoothed expression should be higher where the original expression is higher, and to integrate better with pre-existing PH workflows.

From this surface, we construct a filtered simplicial complex  $(S, f)$ . The nodes of  $S$  are the wells  $[i]$ , and the edges are the  $[i, j]$  where wells  $i$  and  $j$  are adjacent. The index for  $[i]$  is  $z_i$ , and the index for  $[i, j]$  is  $\min\{z_i, z_j\}$ .

Let  $H$  be the 0 dimensional homology of the lower star filtration on  $S$ . The *Coefficient of Spatial Structure* (CoSS) is computed as the  $L^p$  norm of the barcode of  $H$ . By default  $p = 2$ , but this can be altered by the user. A higher  $p$  biases the CoSS to genes with a smaller number of regions with expression much higher than the surrounding tissue.

PersiST also computes a *ratio* statistic as the ratio of the  $L^\infty$  to the  $L^0$  norm of the barcode of  $H$ . This measures how much of the spatial structure in a gene's expression may be explained by a single feature. A sufficiently high value may be indicative of technical artefacts, (*supplementary methods*, supplementary figure 2c,d).

## SVG Calling

PersiST computes a continuous measure of spatial structure for each gene. In our view spatial heterogeneity is a truly continuous quantity and we implore practitioners to treat it as such, but for many tasks it is useful to have a binary yes/no call for whether a gene is SV.

PersiST achieves this by ranking all genes from highest to lowest CoSS, and looking for an “elbow point” in the plot of CoSS versus rank for each gene (figure 1d). All genes with rank below this cutoff  $K$  are declared as SV. PersiST also contains an optional sensitivity parameter  $s$  that enables a practitioner to be more or less permissive about what they wish to consider spatially variable. In this case all genes with rank below  $sK$  are declared SV.

$K$  is computed by looking for the point of maximal curvature in the CoSS-rank plot, using an implementation of the *kneedle* algorithm [25, 26].

## Appendicies

### Data Collection

#### Spatial Transcriptomics Data

For details on the data collection for the kidney and cardiac spatial transcriptomics data sets, see [13] and [14] respectively.

#### MSI Data

For the MSI sample, a Mass spectrometry Imaging experiment was performed on a fresh frozen rat testis sectioned at  $10\mu\text{m}$  of thickness and thaw mounted onto a superfrost glass slide. Desorption Electrospray Ionization (DESI) MSI was carried out using an automated 2D DESI source (Prosolia Inc, Indianapolis, IN, USA) with home-built sprayer assembly mounted to a Q-Exactive FTMS instrument (Thermo Scientific, Bremen, Germany). Analyses were performed at spatial resolutions of  $40\mu\text{m}$  in negative ion mode and mass spectra were collected in the mass range of 80 - 900 with mass resolving power set to 70000 at m/z 200. Individual line scans were converted into centroided .mzML format using MSConvert (ProteoWizard toolbox version 3.0.4043) and subsequently into .imzML using imzML converter v1.3. Mass Imaging data were then uploaded into SCiLS Lab MVS 2024a software (Bruker GmbH, Bremen, Germany) and pixel data from about 2000 m/z features were exported from the software using the SCiLS Lab API and root mean square normalisation.

Haematoxylin and eosin (H&E) staining was performed post MSI analysis on same tissue sections and the stained sections were imaged at 20x with Aperio CS2 digital pathology scanner (Aperio Tech., Oxford, UK), and visualised with Image scope (Aperio Tech., Oxford, UK).

Animal studies were conducted in accordance with UK Home Office legislation, the Animal Scientific Procedures Act 1986, and the AstraZeneca Global Bioethics policy or Institutional Animal Care and Use Committee (IACUC) guidelines. Experimental work outlined in this project has gone through the AstraZeneca Ethical Review Process.

### Availability of data and materials

The kidney disease and myocardial infarction data sets are both publicly available at <https://www.kpmp.org/available-data> and <https://zenodo.org/records/6578047>. For more details, see [13] and [14] respectively.

The code required to run PersiST is available under an Apache 2.0 license at <https://github.com/AstraZeneca/persist>.

## Author contributions statement

J.B. wrote the manuscript, developed the method, implemented it in code and carried out the analysis in this paper. M.C. conceptualised the project. M.C. and I.H. supervised. G.H. and E.C.W. assisted with curation and analysis of the MSI data. R.H. assisted with analysis of the cardiac data. M.S. provided pathologist review for the kidney samples. All authors were involved in the review and editing of the manuscript. All authors have seen and approved the manuscript.

## Acknowledgements

We would like to thank those who worked to generate, organise and share the publicly available spatial transcriptomics datasets analysed in this paper.

## References

- [1] Lambda Moses and Lior Pachter. Museum of spatial transcriptomics. *Nature methods*, 19(5):534–546, 2022.
- [2] Vivien Marx. Method of the year: spatially resolved transcriptomics. *Nature methods*, 18(1):9–14, 2021.
- [3] Natalie Charitakis, Agus Salim, Adam T Piers, Kevin I Watt, Enzo R Porrello, David A Elliott, and Mirana Ramialison. Disparities in spatially variable gene calling highlight the need for benchmarking spatial transcriptomics methods. *Genome Biology*, 24(1):209, 2023.
- [4] Valentine Svensson, Sarah A Teichmann, and Oliver Stegle. Spatialde: identification of spatially variable genes. *Nature methods*, 15(5):343–346, 2018.
- [5] Jiaqiang Zhu, Shiquan Sun, and Xiang Zhou. Spark-x: non-parametric modeling enables scalable and robust detection of spatial expression patterns for large spatial transcriptomic studies. *Genome biology*, 22(1):1–25, 2021.
- [6] Alma Andersson and Joakim Lundeberg. sepal: identifying transcript profiles with spatial patterns by diffusion-based modeling. *Bioinformatics*, 37(17):2644–2650, 2021.
- [7] Gunnar Carlsson. Topology and data. *Bulletin of the American Mathematical Society*, 46(2):255–308, 2009.
- [8] Amanda Rae Buchberger, Kellen DeLaney, Jillian Johnson, and Lingjun Li. Mass spectrometry imaging: a review of emerging advancements and future insights. *Analytical chemistry*, 90(1):240, 2018.
- [9] Larry Wasserman. Topological data analysis. *Annual Review of Statistics and Its Application*, 5:501–532, 2018.
- [10] Abbas H Rizvi, Pablo G Camara, Elena K Kandror, Thomas J Roberts, Ira Schieren, Tom Maniatis, and Raul Rabadan. Single-cell topological rna-seq analysis reveals insights into cellular differentiation and development. *Nature biotechnology*, 35(6):551–560, 2017.
- [11] Raúl Rabadán and Andrew J Blumberg. *Topological data analysis for genomics and evolution: topology in biology*. Cambridge University Press, 2019.

- [12] Katherine Benjamin, Aneesha Bhandari, Zhouchun Shang, Yanan Xing, Yanru An, Nannan Zhang, Yong Hou, Ulrike Tillmann, Katherine R Bull, and Heather A Harrington. Multiscale topology classifies and quantifies cell types in subcellular spatial transcriptomics. *arXiv preprint arXiv:2212.06505*, 2022.
- [13] Blue B Lake, Rajasree Menon, Seth Winfree, Qiwen Hu, Ricardo Melo Ferreira, Kian Kalhor, Daria Barwinska, Edgar A Otto, Michael Ferkowicz, Dinh Diep, et al. An atlas of healthy and injured cell states and niches in the human kidney. *Nature*, 619(7970):585–594, 2023.
- [14] Christoph Kuppe, Ricardo O Ramirez Flores, Zhijian Li, Sikander Hayat, Rebecca T Levinson, Xian Liao, Monica T Hannani, Jovan Tanevski, Florian Wünnemann, James S Nagai, et al. Spatial multi-omic map of human myocardial infarction. *Nature*, 608(7924):766–777, 2022.
- [15] Mathieu Carrière, Steve Y Oudot, and Maks Ovsjanikov. Stable topological signatures for points on 3d shapes. In *Computer graphics forum*, volume 34, pages 1–12. Wiley Online Library, 2015.
- [16] Henry Adams, Tegan Emerson, Michael Kirby, Rachel Neville, Chris Peterson, Patrick Shipman, Sofya Chepushtanova, Eric Hanson, Francis Motta, and Lori Ziegelmeier. Persistence images: A stable vector representation of persistent homology. *Journal of Machine Learning Research*, 18(8):1–35, 2017.
- [17] Ai-Hsien Li, Peter P Liu, Francisco J Villarreal, and Ricardo A Garcia. Dynamic changes in myocardial matrix and relevance to disease: translational perspectives. *Circulation research*, 114(5):916–927, 2014.
- [18] Grégory PA Lacraz, Jan Philipp Junker, Monika M Gladka, Bas Molenaar, Koen T Scholman, Marta Vigil-Garcia, Danielle Versteeg, Hester de Ruiter, Marit W Vermunt, Menno P Creyghton, et al. Tomo-seq identifies sox9 as a key regulator of cardiac fibrosis during ischemic injury. *Circulation*, 136(15):1396–1409, 2017.
- [19] Jan Philipp Junker, Emily S Noel, Victor Guryev, Kevin A Peterson, Gopi Shah, Jan Huisken, Andrew P McMahon, Eugene Berezikov, Jeroen Bakkers, and Alexander van Oudenaarden. Genome-wide rna tomography in the zebrafish embryo. *Cell*, 159(3):662–675, 2014.
- [20] Theodore Alexandrov. Spatial metabolomics: from a niche field towards a driver of innovation. *Nature Metabolism*, 5(9):1443–1445, 2023.
- [21] David S Wishart, AnChi Guo, Eponine Oler, Fei Wang, Afia Anjum, Harrison Peters, Raynard Dizon, Zinat Sayeeda, Siyang Tian, Brian L Lee, et al. Hmdb 5.0: the human metabolome database for 2022. *Nucleic acids research*, 50(D1):D622–D631, 2022.
- [22] A LINK TO CERAMIDE SYNTHASE. Male germ cells require polyenoic sphingolipids with complex glycosylation for completion of meiosis. *Pure Appl. Chem*, 1997(69):2475–2487, 2008.
- [23] Frédéric Chazal, David Cohen-Steiner, and Quentin Mérigot. Geometric inference for probability measures. *Foundations of Computational Mathematics*, 11:733–751, 2011.
- [24] Nina Otter, Mason A Porter, Ulrike Tillmann, Peter Grindrod, and Heather A Harrington. A roadmap for the computation of persistent homology. *EPJ Data Science*, 6:1–38, 2017.

- [25] Ville Satopaa, Jeannie Albrecht, David Irwin, and Barath Raghavan. Finding a "kneedle" in a haystack: Detecting knee points in system behavior. In *2011 31st international conference on distributed computing systems workshops*, pages 166–171. IEEE, 2011.
- [26] Kevin Arvai. kneed - knee point detection in python. URL <https://github.com/arvkevi/kneed?tab=readme-ov-file>.